X-615-68-436

PREPRINT

NASA TM X-63517

THE ROLE OF ATOMIC OXYGEN IN THE IONOSPHERIC E AND F REGION BEHAVIOR

J. R. HERMAN
S. CHANDRA

NOVEMBER 1968

GSFC

GODDARD SPACE FLIGHT CENTER
GREENBELT, MARYLAND

X-615-68-436

THE ROLE OF ATOMIC OXYGEN IN THE IONOSPHERIC E AND F REGION BEHAVIOR

J. R. Herman and S. Chandra

Laboratory for Space Sciences

November 1968

GODDARD SPACE FLIGHT CENTER

Greenbelt, Maryland

PRECEDING PAGE BLANK NOT FILMED.

THE ROLE OF ATOMIC OXYGEN IN THE IONOSPHERIC E AND F REGION BEHAVIOR

J. R. Herman and S. Chandra

Laboratory for Space Sciences

ABSTRACT

The continuity and heat conduction equations for the electron, ion, and neutral gases are solved simultaneously to show the effect of using the heat loss arising from the excitation of the fine structure levels of atomic oxygen, and the heat input from a height dependent electron heating efficiency. The solutions are compared to Thomson backscatter data obtained under conditions similar to those used in the theoretical model. A family of solutions is presented for three different values of the atomic oxygen density at the turbopause level, and compares favorably to certain widely observed features of the main phase of a magnetic storm. From the comparison, it is shown that the results of decreasing the atomic oxygen density at the turbopause level are consistent with the observed changes in both the neutral and ionized constituents relative to quiet magnetic conditions.

PRECEDING PAGE BLANK NOT FILMED.

CONTENTS

THE ROLE OF ATOMIC OXYGEN ON THE IONOSPHERIC

E AND F REGION BEHAVIOR

INTRODUCTION

In a recent paper, Dalgarno and Degges (1968) have shown that an efficient way of cooling the electron gas in the E and F regions of the ionosphere is by the excitation of the fine structure levels of atomic oxygen through inelastic collisions with thermal electrons. This loss process is considerably more important than other elastic and inelastic mechanisms usually considered for construction of theoretical models of the electron temperature. The use of this additional loss term in the electron heat conduction equation offers the possibility of accounting for some of the discrepancies which exist between the theoretically derived electron temperature profiles and those measured by techniques such as Thomson backscatter (Dalgarno et al., 1967 and 1968).

Recently, in presenting the results of the simultaneous solution of the electron continuity equation and the heat conduction equations for the electron, ion, and neutral gases, we briefly discussed the effect of cooling the electron gas through excitation of the atomic oxygen fine structure levels (to be abbreviated hereafter as A.O.F.S. loss). Our result showed that this dominant cooling mechanism has the effect of considerably reducing the electron temperature in the 150 to 250 km altitude range and to a lesser extent elsewhere (Herman and Chandra, 1969; to be referred to as paper I). The purpose of this work is to show the effects of including the A.O.F.S. loss process in the coupled equations for T_e, T_i, T_n, and n_e, and to discuss some of the implications for the general behavior of the F-region.

The Equations of Continuity and Heat Conduction

The continuity and heat conduction equations, their boundary conditions, and the method of obtaining steady state solutions as applied to the F-region ionosphere have been discussed in detail in paper I. For convenience an outline of these equations is presented using the same notation and numerical values.

$$\frac{\partial n_e}{\partial t} = \sum_{j=1}^{3} A_j Q_j - Ln_e^2 + \sin^2 I \frac{\partial}{\partial z} \left\{ \frac{\frac{\partial}{\partial z}\left[n_e k(T_e + T_i)\right] + n_e (m_e + m_i) g}{\sum_{s=1}^{5} \left[m_{O^+} \nu_{O^+s} + m_{es} \nu_{es}\right]} \right\} \quad (1)$$

$$n_e kC_{ve} \frac{\partial T_e}{\partial t} - \sin^2 I \frac{\partial}{\partial z}\left[K_e \frac{\partial T_e}{\partial z}\right] = Q_e - \sum_s L_{es} - L_{ei} - L_{eo}^* \quad (2)$$

$$n_e kC_{vi} \frac{\partial T_i}{\partial t} - \sin^2 I \frac{\partial}{\partial z}\left[K_i \frac{\partial T_i}{\partial z}\right] = L_{ei} - L_i \quad (3)$$

$$N_T k \frac{\partial T_n}{\partial t} - \frac{\partial}{\partial z}\left[K_n \frac{\partial T_n}{\partial z}\right] = Q_n + \sum L_{es} + L_i - L_n + L_{eo}^* \quad (4)$$

$$N_i = \frac{N_i (z_L) T_n (z_L)}{T_n (z)} \exp\left\{- \int_{z_L}^{z} \frac{m_i g(z')}{kT_n (z')} dz'\right\} \quad (5)$$

These equations are the electron continuity equation, the heat conduction equations for electron, ion, and neutral gas temperatures, and the equation of diffusive equilibrium for the neutral gas densities, respectively.

The new term in Equation 2, L^{*}_{eo}, represents the A.O.F.S. loss, and is given by the expression (see appendix)

$$L^{*}_{eo} = \frac{2n_e N_o}{\sqrt{\pi}\, D\left(kT_e\right)^{3/2}} \sqrt{\frac{2}{m_e}} \sum_{\substack{j \\ E_j < E_{j'}}} \sum_{j' \neq j} \left(E_j - E_{j'}\right) g_{j'} \exp\left(-\frac{E_j}{kT_n} - \frac{I_{jj'}}{kT_e}\right)$$

$$\cdot \left[1 - \exp\left(-\frac{I_{jj'}}{kT_e T_n}\left(T_e - T_n\right)\right)\right] \int_0^{\infty} E' \sigma_{eo}\left(j' \rightarrow j, E'\right) e^{-E'/kT_e}\, dE' \quad (6)$$

where

n_e = the electron density

N_o = the atomic oxygen density

m_e = the electron mass

T_e, T_i, T_n are the electron, ion, and neutral temperatures

k = Boltzmann's constant

E_j = the j^{th} fine structure energy level of atomic oxygen corresponding to the angular momentum quantum number j

$I_{jj'} = E_{j'} - E_j$

$g_j = 2j + 1$

$\sigma_{eo}(j' \rightarrow j, E')$ = the cross section for downward transitions from j' to j

$$D = \sum_{j'} g_{j'} \exp\left(-E_{j'}/kT_n\right)$$

Equation 6 has been obtained by combining the terms for upward and downward transitions using detailed balance and then averaging over the Maxwellian velocity distribution of the electrons. In addition, it is assumed that the population of atomic oxygen fine structure energy levels is given by the Boltzmann distribution at temperature T_n. When the numerical values for σ_{eo} ($j' \rightarrow j$, E'), given by Breig and Linn (1966), are used, the following numerical approximation to (6) is obtained (see appendix)

$$L^*_{eo} = \left(5.56 - 2.40 \times 10^{-4}\, T_n\right)\left(6.23 + 2.75 \times 10^{\text{[illegible]}}\, T_n\right)$$

$$\times\ 10^{-25}\, n_e\, N_o \left(T_e - T_n\right) \big/ T_n \ \text{ergs cm}^{-3}\ \text{sec}^{-1} \qquad (7)$$

which agrees approximately with the values given by Dalgarno and Degges (1968).

For Equations 1 to 5 the heating and ionization efficiencies are available as free parameters if adjustments are needed for comparison with data. With the use of Equation 7 it was felt that the ionization efficiency should be taken as 1.0 (see paper I) along with two cases of the electron heating efficiency. The heat production function, Q_e, is obtained by computing the production rate of electron-ion pairs and multiplying by a constant (with altitude) heating efficiency of 2.5 ev per electron ion pair. Since this procedure underestimates the heating rate in the high altitude range, a height dependent electron heating efficiency suggested by Dalgarno et al. (1968), and approximated by the values shown in Figure 1, is used for comparison with the constant efficiency.

DISCUSSION

The results of solving Equations 1 to 5 with and without the A.O.F.S. loss and the height dependent electron heating efficiency are shown in Figure 2. The parameters used for this case correspond to low solar activity (HF* = 0.9),* afternoon conditions (time = 13:30 hours), latitude and dip approximating Arecibo, Puerto Rico (Lat = 18° and Dip = 50°), and for the solar declination angle computed for September 22. In addition, the boundary conditions for the neutral gas density at 100 km were taken as $[N_2] = 4.65 \times 10^{12}$, $[O_2] = 1.25 \times 10^{12}$, $[O] = 7.50 \times 10^{11}$, $[H_e] = 2.50 \times 10^{8}$, and $[H] = 1.00 \times 10^{5}$ cm^{-3}.

The most significant change occurs in the vicinity of 190 km where the high peak electron temperature is reduced by 50%. When only the A.O.F.S. loss is used, the significant temperature changes are confined to the lower altitudes below about 300 km as is shown in Figure 2 (curve 2). However, with the height dependent electron heating efficiency and the A.O.F.S. loss, the high altitude electron temperature is enhanced by about 30% (see curve 3). The temperature enhancement is in turn reflected in a considerable change in the slope of the electron density profile above h_m F2. The higher temperature in the region where diffusion is important produces the change in n_e shown in the upper portion of curve 3. The large decrease in T_e below 300 km produces only a small change in n_e, since here the electron density profile is largely determined by chemical processes and not diffusion. The introduction of the A.O.F.S. loss does shift h_m F2 downward by about 30 km with a slight increase in h_m F2, and also causes a decrease in layer thickness.

The abbreviation HF = N stands for the solar flux values in the spectral range of 10 to 1027 A, as given by Hinteregger et al. (1965), multiplied by N.

Since the heat input from the electron to the neutral gas amounts to about 15% of the total, it might be expected that the addition of the A.O.F.S. loss would add to this heat input. The neutral gas temperatures corresponding to the curves of Figure 2 do not show such an effect (T_∞ (1) = 887°K, T_∞ (2) = 870°K since the heat input from the electron gas below about 300 km is largely determined by the magnitude of Q_e. That is, with the addition of the A.O.F.S. loss the electron temperature adjusts itself downward until the heat loss rate to the other gases is about the same as before (Q_e is almost uneffected by A.O.F.S. loss). Above about 400 km, where T_e is not controlled by the A.O.F.S. loss, the electron temperature shows only a very small increase due mainly to the small decrease in electron density and neutral temperature (compare curves 1 and 2). This is borne out by curve 3 (T_∞ (3) = 925°K), where the increased heat input at almost all altitudes, compared to curve 2, results in a higher value of T_e and T_n in spite of increased n_e.

For quantitative comparison of the present theoretical models with observational data, it is necessary to simultaneously measure the density and temperature of both ionized and neutral constituents along with the solar EUV flux. In the case of Thomson backscatter, the quantities that are usually measured are the charged particle temperatures and densities. The information about the solar EUV flux and the neutral gas composition have to be inferred independently from solar decimeter flux, satellite drag, and atmospheric models. With this limitation in view, it is meaningful to compare the theoretical results with the

Thomson backscatter data whenever the conditions during the experiment are reasonably close to those used in the present calculation. An example of equinoctial midday data taken during a time of low solar activity (Sept. 22, 1965 at 13:15) has been presented by Mahajan* (1967), and is reproduced in Figure 3. A comparison with the curves labelled 3 in Figure 2 (redrawn in Figure 3) shows a sufficient similarity to indicate that the introduction of the A.O.F.S. loss and the height dependent electron heating efficiency are necessary for obtaining satisfactory ionospheric models.

Another example of simultaneous electron density and temperature measurements from Thomson backscatter has been given by Rao (1968) for July 28, 1965 at 15:00 hours (not reproduced here). The conditions for this data roughly correspond to the same solar zenith angle and solar activity as adopted in Figure 2. In this and other similar data taken under conditions that are well enough known to be compared to the models, the main features are well reproduced for the T_e, T_i, and n_e profiles. In addition to the magnitudes of T_e, T_i, and n_e, both the data and the theoretical models show a decrease in the logarithmic slope with increasing altitude whenever there are substantial electron temperature gradients above h_m F2. A similar change in the logarithmic slope can occur when there are changes in the ionic composition from O^+ to H^+. However, it is reasonable to assume that the ionic composition was mainly O^+ until above about 750 km for the data taken on July 28, 1965 during the afternoon, and therefore

*The electron density profile shown in Figure 3 is unpublished, and has been kindly provided by the author for comparison.

the decrease in the magnitude of the logarithmic slope can be attributed to the electron temperature gradient.

THE EFFECTS OF VARIABLE [O]

The effects of changing the atomic oxygen density boundary values have been discussed previously in the absence of A.C F.S. loss and the height dependent electron heating efficiency (paper I also Chandra and Herman, 1969; to be referred to as paper II). With the introduction of the A.O.F.S. loss, both the neutral and electron gas temperatures are directly controlled by the atomic oxygen density. Changes in [O], either through dynamic or chemical processes, can be expected to have profound effects on the E and F-region ionosphere

As expected, the use of the A.O.F.S. loss and the height dependent electron heating efficiency did not change any of the essential conclusions presented in either paper I or paper II, even though the details of the T_e, T_i, T_n, and n_e profiles are substantially different. Figure 4 shows a family of profiles obtained by setting the atomic oxygen density at 100 km to 1.00×10^{12}, 7.50×10^{11}, and 5.00×10^{11} for curves A, B, and C respectively. The remaining parameters have been held constant (for this case the parameters correspond to low solar activity (HF* = 1.00), midday conditions (time = 12:00 hours), latitude and dip corresponding to Wallops Island, Virginia (Lat = 37° and Dip = 70°), and for the solar declination angle computed for March 2.

If, as discussed in paper II, the conditions well after the onset of a magnetic storm are characterized by a decrease in the atomic oxygen density at the turbopause level, then curves A, B, and C can be interpreted as corresponding to quiet, disturbed, and very disturbed conditions, respectively. The commonly known changes in the F-region parameters in the middle and high latitudes associated with the main phase of a magnetic storm are given in the following list.

1. A decrease in foF2 (up to 50%).
2. An increase in h_m F2 (up to 100 km).
3. An increase in the topside electron density from about 100 km above the F2 peak.
4. A decrease in the total electron content.
5. A worldwide increase in satellite drag that can be interpreted as an increase in both neutral temperature and density.

These features of a magnetic storm, as referred to quiet conditions (curve A), are clearly shown in Figure 4. In addition, the exospheric neutral temperature increased by over 200°K $\left(T_\infty (A) = 796°K, T_\infty (B) = 888°K, \text{and } T_\infty (C) = 1000°K\right)$ accompanied by an increase in the total neutral density at all heights. Also, as would be expected, the effect of decreasing atomic oxygen is to increase both the electron and ion temperatures and the height of the T_e maximum. The main difference between this and the previous description of a magnetic storm by Chandra and Herman (1969) is in the magnitudes of the resulting temperatures and densities. Specifically, the rarely observed sharp peaks in the electron temperature no longer appear, the gradients in both the electron temperature and electron density above 300 km increase, and the ion temperatures are considerably increased above 450 km where T_i begins to tend strongly towards T_e and away from T_n (note, however, that T_i does not become equal to T_e for the altitude range considered, 100 to 1000 km).

SUMMARY

The equations of heat conduction for the electron, ion, and neutral gases have been solved simultaneously with the electron continuity equation using the A.O.F.S. loss process and a height dependent heating efficiency. The resulting solutions show that the electron temperature is significantly reduced below about 300 km where the A.O.F.S. loss is most important and increased at higher altitudes because of the increased heat input from the height dependent electron heating efficiency. Smaller changes take place in the electron density profile and the height of the maximum, $h_m F2$, because of the reduced electron temperature and gradients entering into the diffusion velocity. Finally, the ion temperature is increased in proportion to the increased electron temperature.

The comparison of these solutions with Thomson backscatter data show that the changes brought on by including the A.O.F.S. loss and the height dependent electron heating efficiency remove some of the qualitative and quantitative discrepancies between the theoretical and measured profiles.

A family of profiles are presented for T_e, T_i, and n_e for three different values of the neutral atomic oxygen density boundary condition at the turbopause

level. These results compare favorably with certain widely observed features i.. the F-region appearing well after the onset of a magnetic storm. From this agreement it can be concluded that most of the observations can be explained by a decrease in the atomic oxygen density at the turbopause level relative to quiet magnetic conditions.

REFERENCES

1. Breig, E. L. and C. C. Linn, 1966, Phys. Rev., 151, 67.
2. Chandra, S. and J. R. Herman, 1969, Planet. Space Sci., to be published.
3. Dalgarno, A. and T. C. Degges, 1968, Planet. Space Sci., 16, 125.
4. Dalgarno, A., M. B. McElroy, M. H. Rees, J. C. G. Walker, 1968, preprint.
5. Herman, J. R. and S. Chandra, 1969, Planet. Space Sci., to be published.
6. Hinterreger, H., L. Hall, and G. Schmidtke, 1965, Space Research V, 1175.
7. Mahajan, K. K., 1967, J. Atoms. Terr. Phys., 29, 1137.
8. Rao, P. B., 1968, J. Geophys. Res., 73, 1661.

PRECEDING PAGE BLANK NOT FILMED.

APPENDIX

Consider a gas, each atom of which possesses internal energy eigenvalues E_i, interacting via inelastic collisions with an electron gas so as to cause transitions between the states E_i and E_j. Assume the gases to have kinetic energy distributions $f_e(E_e)$ and $f_a(E_a)$, cross sections for the transitions between E_i and E_j of $\sigma_e(i \to j, E)$ and $\sigma_a(i \to j, E)$, for electron-atom and atom-atom collisions respectively, and that the state E_i has an occupation number n_i. The number of transitions into the state i per unit volume per second is given by

$$\frac{dn_{ij}}{dt} = -\int d^3 v_e \int d^3 v_a\, n_i\, f_e\, f_a \left|\vec{v}_e - \vec{v}_a\right| \sigma_e(i \to j) + \int d^3 v_e \int d^3 v_a\, n_j\, f_e\, f_a \left|\vec{v}_e - \vec{v}_a\right|$$

$$\cdot\, \sigma_e(j \to i) - \int d^3 v_a' \int d^3 v_a\, n_i\, f_a(v_a)\, f_a(v_a')\, \sigma_a(i \to j) \left|\vec{v}_a - \vec{v}_a'\right|$$

$$+ \int d^3 v_a' \int d^3 v_a\, f_a(v_a)\, f_a(v_a')\, n_j\, \sigma_a(j \to i) \left|\vec{v}_a - \vec{v}_a'\right| \qquad \text{(A1)}$$

Since $\sigma(i \to j)$ is assumed to depend only on the magnitude of the relative velocity, some of the integrals may be evaluated to yield

$$\frac{dn_{ij}}{dt} = +N_a \left[-\int_{I_{ij}}^{\infty} dE\, f_e(E)\, n_i \sqrt{\frac{2E}{m_e}}\, \sigma_e(i \to j, E) + \int_0^{\infty} dE\, f_e(E) \sqrt{\frac{2E}{m_e}}\, n_j\, \sigma_e(j \to i, E) \right.$$

$$\left. - \int_{I_{ij}}^{\infty} dE\, f_a(E)\, n_i \sqrt{\frac{4E}{m_a}}\, \sigma_a(i \to j, E) + \int_0^{\infty} dE\, f_a(E)\, n_j \sqrt{\frac{4E}{m_a}}\, \sigma_a(j \to i, E) \right] \qquad \text{(A2)}$$

where $I_{ij} = E_j - E_i$, $f_a(E)$ is Maxwellian, $\left|\vec{v}_a - \vec{v}_a'\right| = \sqrt{4E/m_a}$, and m_e and m_a are the electron and atom masses respectively.

During the inelastic collision only one of the particles is assumed to undergo an internal energy change while the other changes its kinetic energy from E to E′. Detailed balance can now be used to relate the upward and downward transition cross sections.

$$E\, g_i\, \sigma(i \to j, E) = E'\, g_j\, \sigma(j \to i, E') \tag{A3}$$

where g_i is the degeneracy of the i^{th} state. If it is assumed that $E_j > E_i$, then the rate at which electrons lose energy to the atoms per unit volume is

$$L^*_{ea} = \sum_{i} \sum_{\substack{j \neq i \\ E_j > E_i}} \left(E_j - E_i\right) \frac{dn_{ij}}{dt} \tag{A4}$$

Using A3 to combine the integrals in A2 by eliminating $\sigma_e(i \to j, E)$, assuming f_e to be Maxwellian at a temperature T_e, and assuming that the electron collisions are infrequent enough so that the occupation number n_j can be well approximated by the Boltzmann distribution

$$n_j = \frac{1}{D}\, g_j \exp\left(-E_j/kT_a\right) \tag{A5}$$

Equation A4 becomes

$$L_{ea}^{*} = \frac{2}{D\sqrt{\pi}} \frac{n_e N_a}{(kT_e)^{3/2}} \sqrt{\frac{2}{m_e}} \sum_{i} \sum_{\substack{j \neq i \\ E_j > E_i}} (E_j - E_i)\, g_j \exp\left(-\frac{E_j}{kT_a} - \frac{I_{ij}}{kT_e}\right)$$

$$\cdot \left[1 - \exp\left(-\frac{I_{ij}}{kT_e T_a}(T_e - T_a)\right)\right] \int_0^{\infty} E\sigma_e(j \to i, E)\, e^{-E/kT_e}\, dE \cdot \qquad \text{(A6)}$$

(A6 is an alternate form to that given by Dalgarno and Degges, 1968), where n_e and N_a are the electron and atom number densities respectively, and D is given by

$$D = \sum_{j} g_j \exp\left(-E_j/kT_a\right) \qquad \text{(A7)}$$

When the numerical values for $\sigma_e(j \to i, E)$ are used, as given by Breig and Linn (1966), the cross sections can be represented by the form

$$\sigma_e(j \to i, E) = A_{ij} E^2 + B_{ij} E + C_{ij} \qquad (E < kT_o) \qquad \text{(A8)}$$

$$\sigma_e(j \to i, E) = \sigma_o \qquad (E \geq kT_o) \qquad \text{(A9)}$$

$$\sigma_e(j \to i, E) = kT_o\, \sigma_o/E \qquad (E \geq kT_o) \qquad \text{(A10)}$$

where kT_o represents an electron kinetic energy above which the cross sections are assumed to be a constant value σ_o or to decrease with a 1/E energy dependence.

The result of using Equations A8 and A9 to evaluate A6 is

$$L^{*}_{eo} = \frac{2n_e N_a}{D\sqrt{\pi}} \sqrt{\frac{2k\,T_e}{m_e}} \sum_{\substack{j \\ E_j > E_i}} \sum_{i \neq j} \left(E_j - E_i\right) g_j \exp\left(- \frac{E_j}{kT_a} - \frac{I_{ij}}{kT_e}\right)$$

$$\cdot \left[1 - \exp\left(- \frac{I_{ij}}{kT_e\,T_a} \left(T_e - T_a\right)\right)\right] F_{ij} \qquad \text{(A11)}$$

$$F_{ij} = \Big[6A_{ij}\left(kT_e\right)^2 + 2B_{ij}\left(kT_e\right) + C_{ij} + \Big\{\sigma_o\left(X_o + 1\right) - A_{ij}\left(kT_e\right)^2\left(X_o^3 + 3X_o^2\right.$$

$$\left. + 6X_o + 6\right) - B_{ij}\left(kT_e\right)\left(X_o^2 + 2X_o + 2\right) - C_{ij}\left(X_o + 1\right)\Big\} e^{-X_o}\Big] \qquad \text{(A12)}$$

$$X_o \equiv kT_o/\left(kT_e\right)$$

If instead, A10 is used in place of A9, the term $X_o\,\sigma_o$ replaces $\sigma_o\left(X_o + 1\right)$. For the case of A.O.F.S. loss, the values of A_{ij} , B_{ij} , and C_{ij} are taken to be (for σ_e in units of the Bohr area, πa_o^2, and E in ergs)

A_{10}	=	-1.400×10^{24}	B_{10}	=	2.944×10^{12}	C_{10}	=	0.3093
A_{21}	=	-9.171×10^{23}	B_{21}	=	1.978×10^{12}	C_{21}	=	0.5426
A_{20}	=	-8.814×10^{23}	B_{20}	=	1.844×10^{12}	C_{20}	=	0.2588

Inserting these values in Equation A11 and performing the indicated summations for $i = 1, 2, 3$ and $j = 1, 2, 3$ give the following approximation for L^*_{eo},

$$L^*_{eo} = (5.56 - 2.40 \times 10^{-4} T_e)(6.23 + 2.75 \times 10^{-3} T_n)$$

$$\times 10^{-25} n_e N_o (T_e - T_n)/T_n \text{ ergs cm}^{-3} \text{ sec}^{-1} \qquad \text{(A13)}$$

When Equation A10 is used in place of A9, the same values (within 2%) of L^*_{eo} are obtained for electron temperatures less than 2500°K. Above this temperature the results slowly diverge to produce values that are lower by as much as a factor of 1.8 when $T_e = 11,000$°K.

FIGURE CAPTIONS

Figure 1. Height dependent electron heating efficiency.

Figure 2. A comparison of constant heating efficiency without A.O.F.S. loss (curve 1) with constant heating efficiency with A.O.F.S. loss (curve 2) and height dependent electron heating efficiency with A.O.F.S. loss (curve 3).

Figure 3. Thomson backscatter results for September 22, 1965 (13:15 hours) at Arecibo, Puerto Rico (Mahajan, 1967).

Figure 4. The effect of varying the density of neutral atomic oxygen at the lower boundary (100 km). Curve A — $[O] = 1.00 \times 10^{12}$, curve B — $[O] = 7.50 \times 10^{11}$, and curve C — $[O] = 5.00 \times 10^{11}$ cm^{-3}.

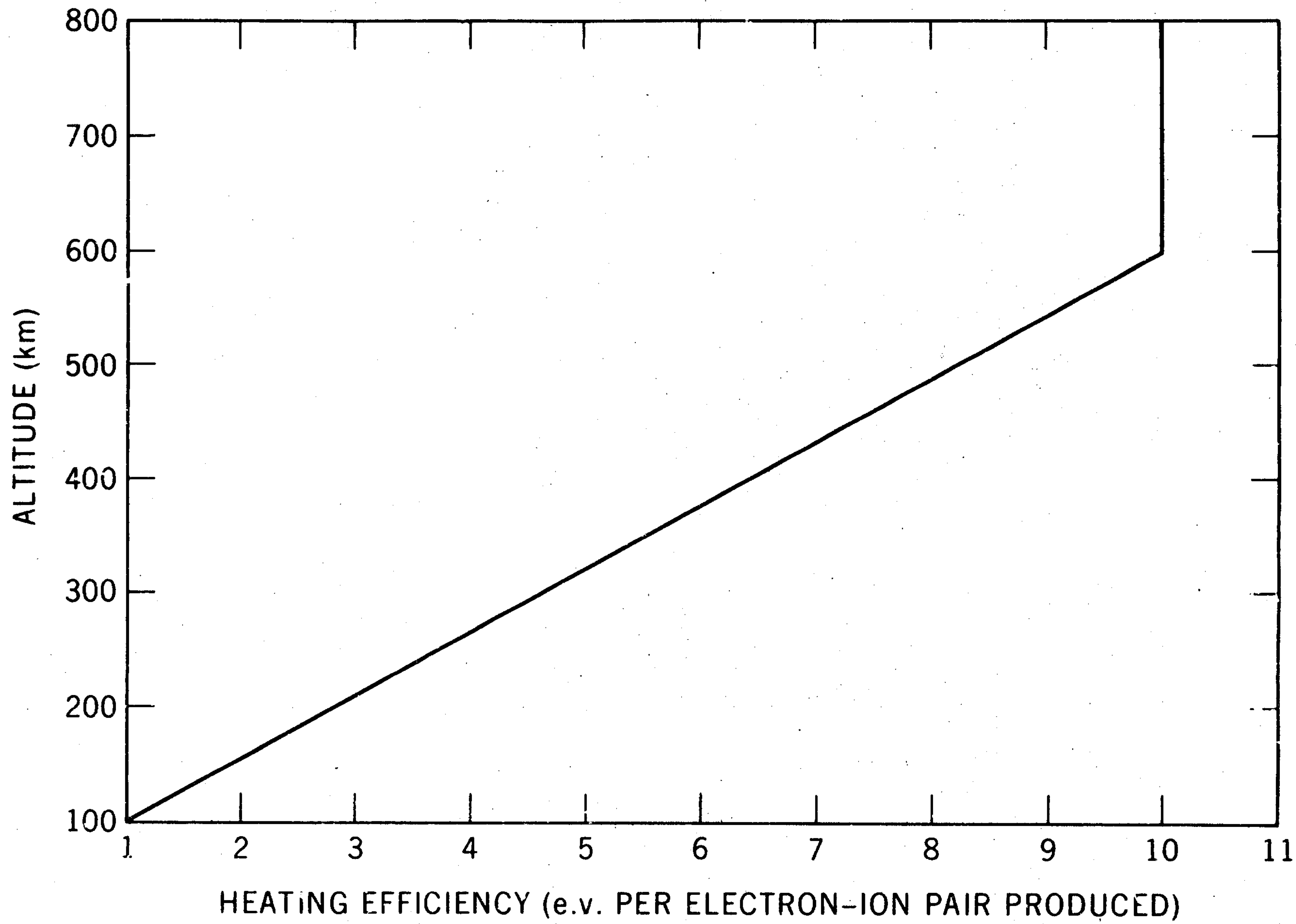
ALTITUDE (km)
800
700
600
500
400
300
200
100
1
2
3
4
5
6
7
8
9
10
11
HEATiNG EFFICIENCY (e.v. PER ELECTRON-ION PAIR PRODUCED)

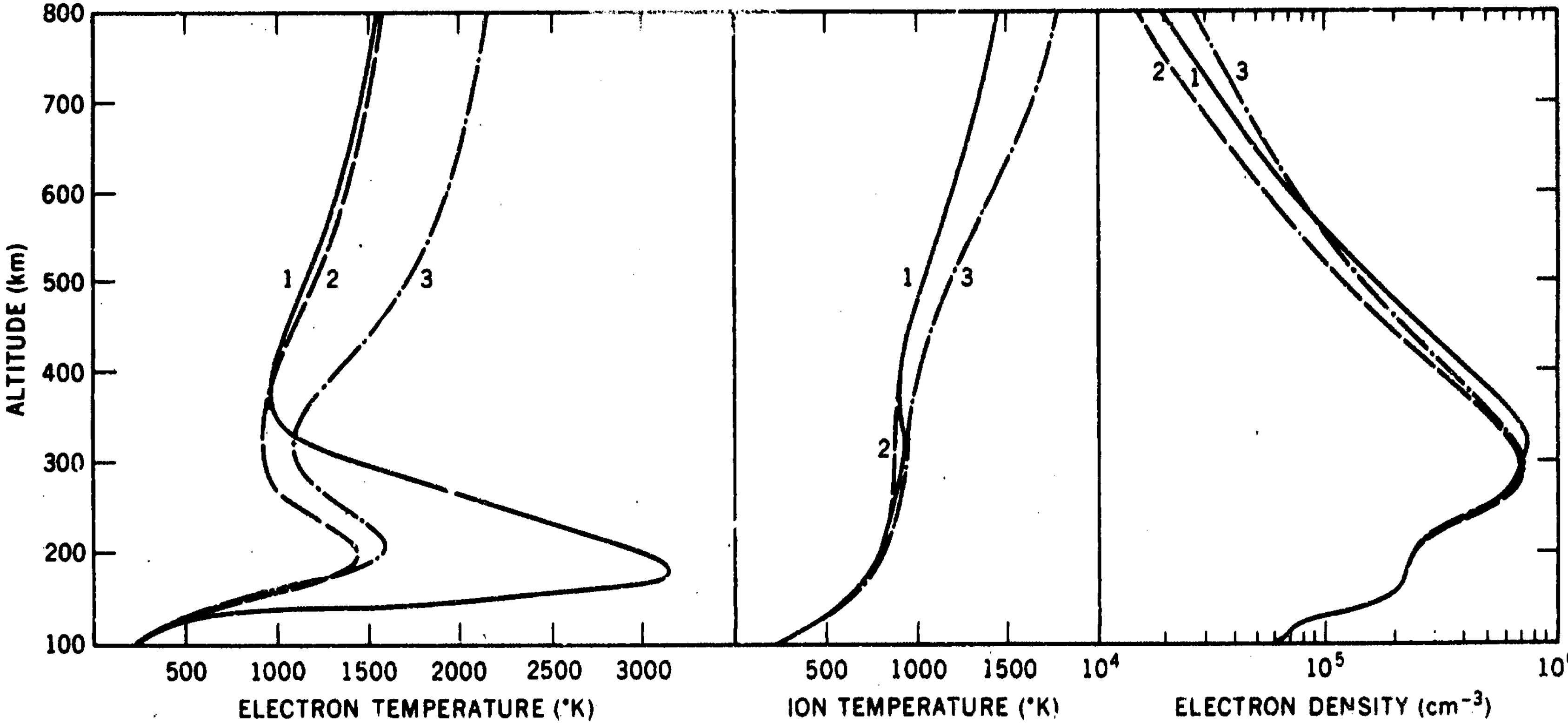
ALTITUDE (km)
800
700
600
500
400
300
200
100
500
1000
1500
2000
2500
3000
ELECTRON TEMPERATURE (°K)
ION TEMPERATURE (°K)
10^4
10^5
10^6
ELECTRON DENSITY (cm^-3)
1
2
3

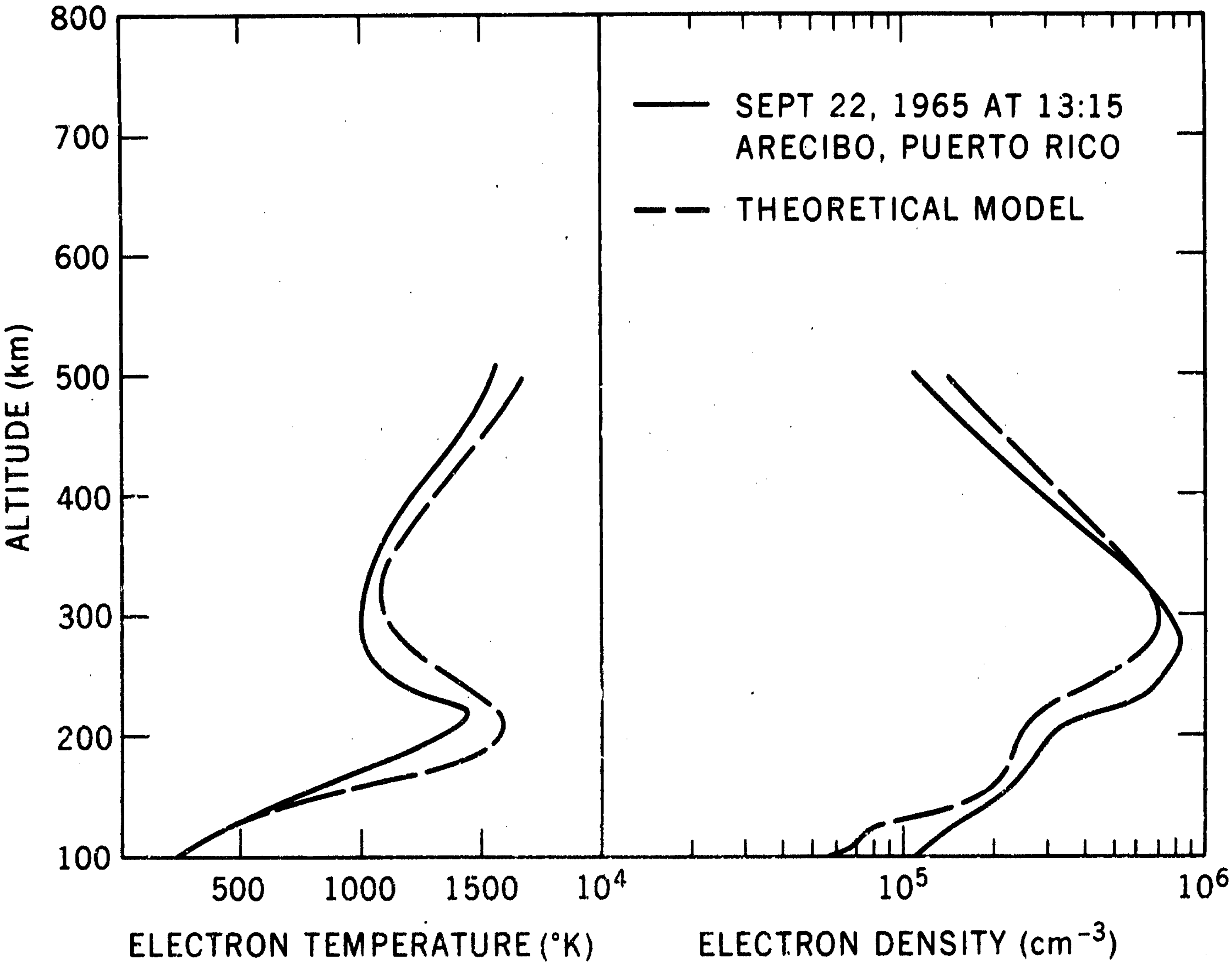

SEPT 22, 1965 AT 13:15
ARECIBO, PUERTO RICO
THEORETICAL MODEL
ALTITUDE (km)
800
700
600
500
400
300
200
100
500
1000
1500
10^4
10^5
10^6
ELECTRON TEMPERATURE (°K)
ELECTRON DENSITY (cm^-3)

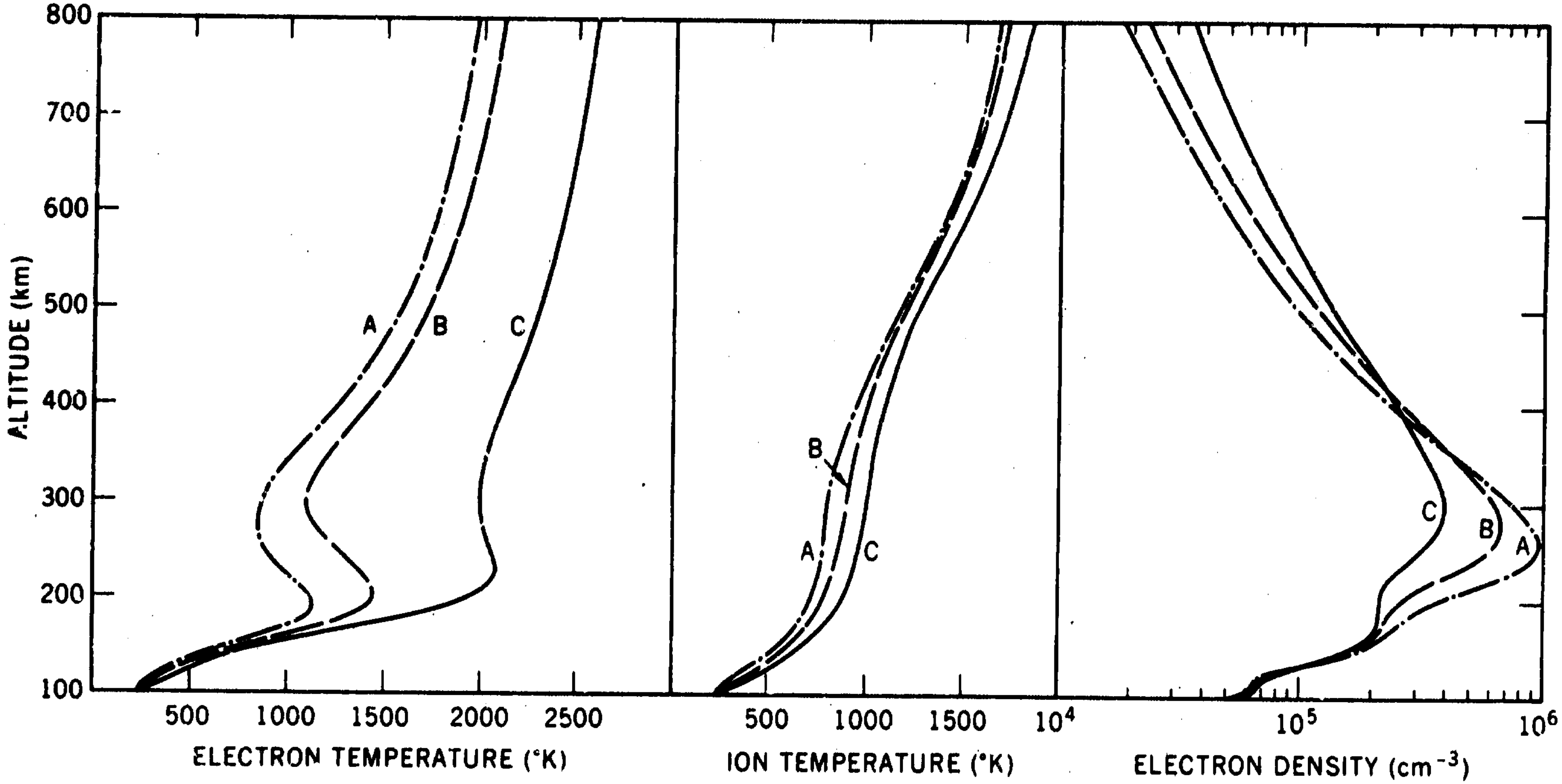
800
700
600
500
400
300
200
100
ALTITUDE (km)
A
B
C
500
1000
1500
2000
2500
ELECTRON TEMPERATURE (°K)
B
A
C
500
1000
1500
10^4
ION TEMPERATURE (°K)
C
B
A
10^5
10^6
ELECTRON DENSITY (cm^{-3})